Extensive investigation into ductile-iron natural gas pipeline corrosion in soils

Fumio Kajiyama, Dr.
Tokyo Gas Pipeline Co., Ltd., 1-5-20, Kaigan, Minato-ku, Tokyo 105-8527, Japan

Abstract

In Japan, ductile-iron pipelines have been used widely for more than 65 years as water and gas pipelines because of the superior strength and toughness. This paper summarizes evaluations conducted in the Tokyo metropolitan area for ductile-iron natural gas pipelines where neither polyethylene encasement nor cathodic protection was included at the time of construction and thereafter; therefore, investigated pipelines were primarily under the influence of corrosivity of soils. Corrosion fell into three divisions roughly according to pH range of soil, that is, 1) acid corrosion caused by iron-oxidizing bacteria at pH below 5, 2) sulfate-reducing bacteria corrosion at pH 5 to 9,5, and 3) HCO_3^-−CO_3^{2-} corrosion at pH 8 to 12. Heterogeneous soils likely increased the risk of differential aeration attack. It was considered that insoluble iron hydroxide formed on a pipe surface dissolved by a large amount of HCO_3^-, resulting in corrosion at pH above 8 in aerobic soils. Stray-current corrosion was observed in a d.c. stray current exposure area.

1 Introduction

Ductile-iron has superior strength and ductility to grey-iron, so mechanical failure was reduced. The superior physical properties allowed manufacturers to reduce the wall

thickness to over 50 % of equivalent grey-iron. In Tokyo metropolitan area, many corrosion failures of ductile-iron pipes have occurred in acid sulfate soils, reclaimed lands, and sandy marine sediments where the risk of microbially influenced corrosion was increased. In this investigation into ductile-iron natural gas pipeline corrosion in soils, particular emphasis was placed on the effect of microorganisms (Iron-oxidizing bacteria, sulfate-reducing bacteria, and iron bacteria) on the corrosion.

2 Field surveys

A total of 354 locations were selected for investigation based upon leakage history, burial years and environment. After excavating and removing corrosion products and soil adhered to the pipe surface, corrosion depth measurement was made using depth gage. Maximum corrosion rate was recorded.

3 Soil and corrosion product analyses and on-site measurements

An attempt has been made to pinpoint the physical and chemical factors that influence corrosion in soils. Soil samples and corrosion products were taken from each site in the vicinity of the site showing maximum corrosion depth and specific gravity, resistivity, the pH, Eh, soluble ion (Fe^{2+}, SO_4^{2-}, Cl^-, HCO_3^-) and iron sulfide contents, and microbiological assay were measured by the method already described [1].

Soil was weighed immediately after sampling (mass of wet soil) , after that dried for 24 hours at 110℃ and weighed again (mass of dry soil). Water content, W_c was calculated from the following equation (1):

Water content, W_c
= {(mass of wet soil) – (mass of dry soil)}／(mass of dry soil)} × 100 (1)

Bacterial enumeration of iron-oxidizing bacteria, sulfur-oxidizing bacteria, and sulfate-reducing bacteria was by standard Most Probable Number Technique. It should be noted that iron-oxidizing bacteria can proliferate in acid environment, whereas iron bacteria can grow in neutral environment.

Corrosion potential of ductile-iron test specimen having a surface area of 6 cm^2 together with pipe-to-soil potential was measured on site. The aeration characteristics of a soil are dependent primarily upon physically characteristics such as the particle size and its distribution. Corrosion potential is a reliable indication of the effect of

aeration characteristics on the pipeline. As corrosion potential is more negative, the soil becomes more anaerobic.

4 Results and discussion

4.1 Controlling factors for redox potential

The author reported that the redox potential Eh decreases with increase in pH and soluble ferrous ion concentration [Fe^{2+}] for a total of 373 soil samples in the Tokyo metropolitan area. Eh is statistically expressed by the following equation (2):

The author reported that Eh was determined by pH and soluble ferrous concentration, according to the equation (2) [2]:

$$Eh = 0{,}803 - 0{,}0496\ pH - 1{,}55\ [Fe^{2+}] \quad (2)$$

where

Eh : redox potential V_{SHE}

$[Fe^{2+}]$: soluble ferrous ion concentration, 0 − 0,3028 mol / L

It must be emphasized that the soluble ferrous ion concentration is important in governing the Eh which relates to the activities of bacteria.

Figure 1 shows the relationship between measured Eh and estimated Eh obtained from the multiple regression equation (2). It was proved that a multiple coefficient factor is 0,794 which indicates Eh is expressed by pH and soluble ferrous ion concentration.

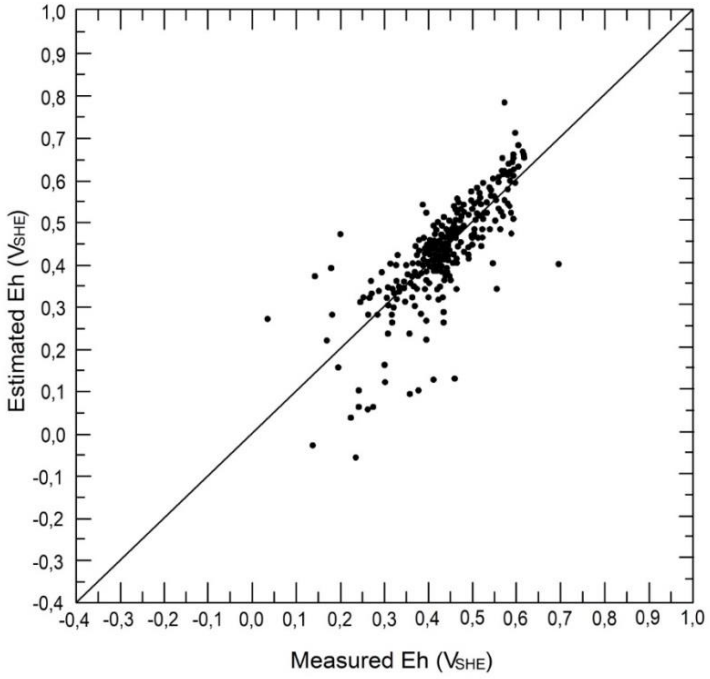

Figure 1 Relationship between measured Eh and estimated Eh obtained from the multiple regression equation (2).

4.2 Relationship between maximum corrosion rate and soil pH

It is convenient and traditional to express corrosion rate as millimeters per year (mm/y) to provide an indication of penetration. Maximum corrosion rate was obtained from (maximum corrosion depth)／(years in service).

Figure 2 shows the relationship between soil pH and maximum corrosion rate higher than 0,3 mm/y. Plots with upward red arrow indicated that pits were discovered after removal of corrosion products and soil adhered to the pipe surface.

It should be noted that ductile-iron pipe can corrode at any pH, although different rates of that corrosion were observed.

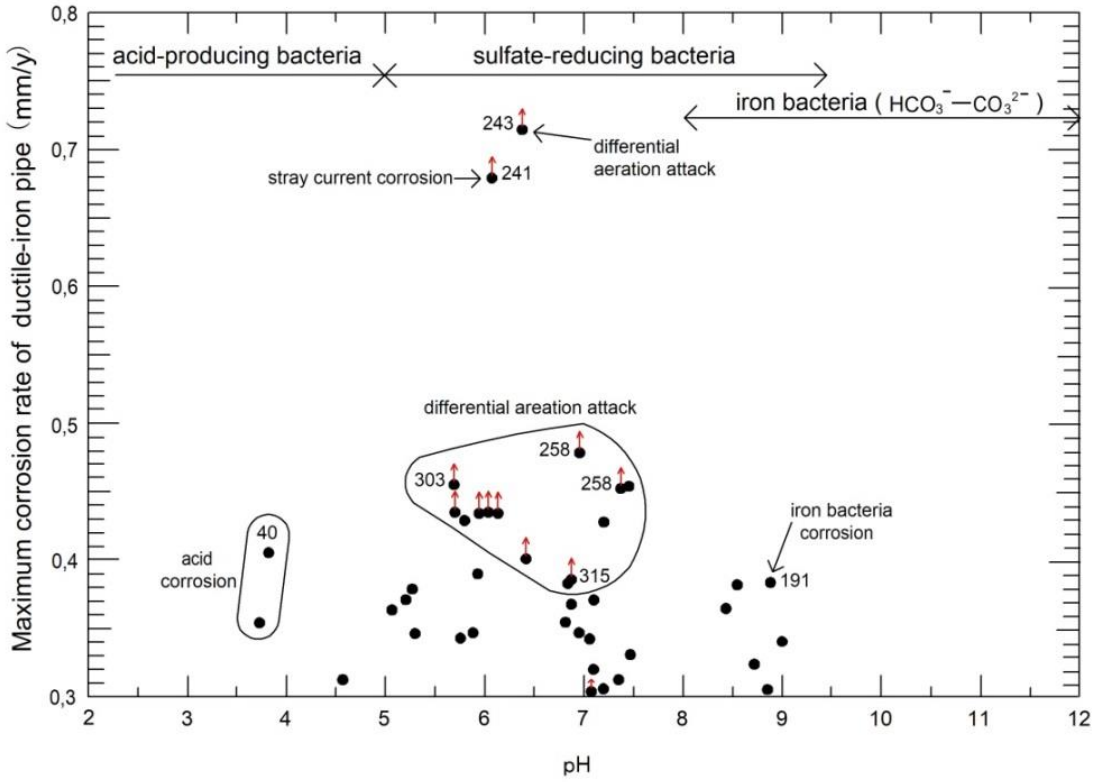

Figure 2 Relationship between soil pH and maximum corrosion rate higher than 0,3 mm/y of ductile-iron pipe. Numbers stand for serial number of the investigation.

4.3 Corrosion potential of ductile-iron test specimen as an indication of aeration characteristics

Figure 3 shows the relationship between corrosion potential of ductile-iron test specimen and water content. In the case of water content greater than 100 %, all the corrosion potentials were more negative than −0,80 V_{CSE}, indicating anaerobic soil and fixed anodic sites.

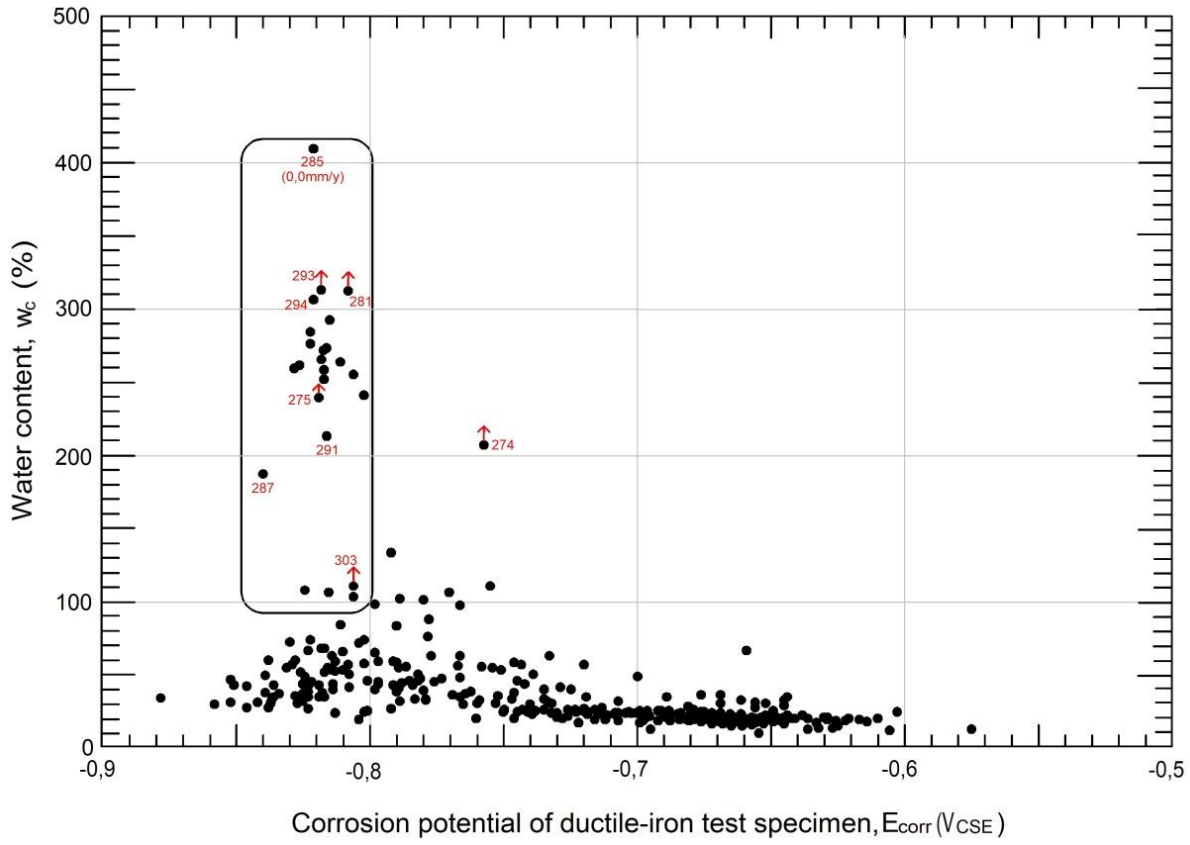

Figure 3 Relationship between corrosion potential of ductile-iron test specimen and water content.

4.4 Causes of ductile-iron pipeline corrosion

4.4.1 Differential aeration attack in heterogeneous soil (No. 243)

Heterogeneous soils can affect corrosion by creating differential aeration cells on the pipe surface and fixing the location of anodic sites having more negative corrosion potentials of ductile-iron test specimens.

Corrosion failure occurred buried in a mixture of clay and sand. This pipe had been in service for 13 years. Maximum corrosion rate was more than 0,715 mm/y. Heterogeneous soil caused differential aeration attack.

4.4.2 Corrosion in a d.c. stray current exposure area (No. 241)

An investigation into a natural gas low pressure 100 mm diameter line with cover of 3 m was made. This pipe had been in service for 14 years when three corrosion pits were discovered after removal of corrosion products and soil adhered to the pipe surface. Graphitic corrosion was observed.

As this pipeline was buried near d.c. transit system, pipe-to-soil measurements were made along the line and on both sides of it at intervals of 20 cm as shown in Figure 4.

The position of copper sulfate electrode was marked with ○. The effects of d.c. transit system can cause observation of marked and extreme variations in pipe-to-soil potential values. The variation was from −7 to −398 millivolts with respect to the copper sulfate electrode. Tree corrosion pits were deemed to have been caused by d.c. stray current after a comprehensive investigation eliminated all other possible causes.

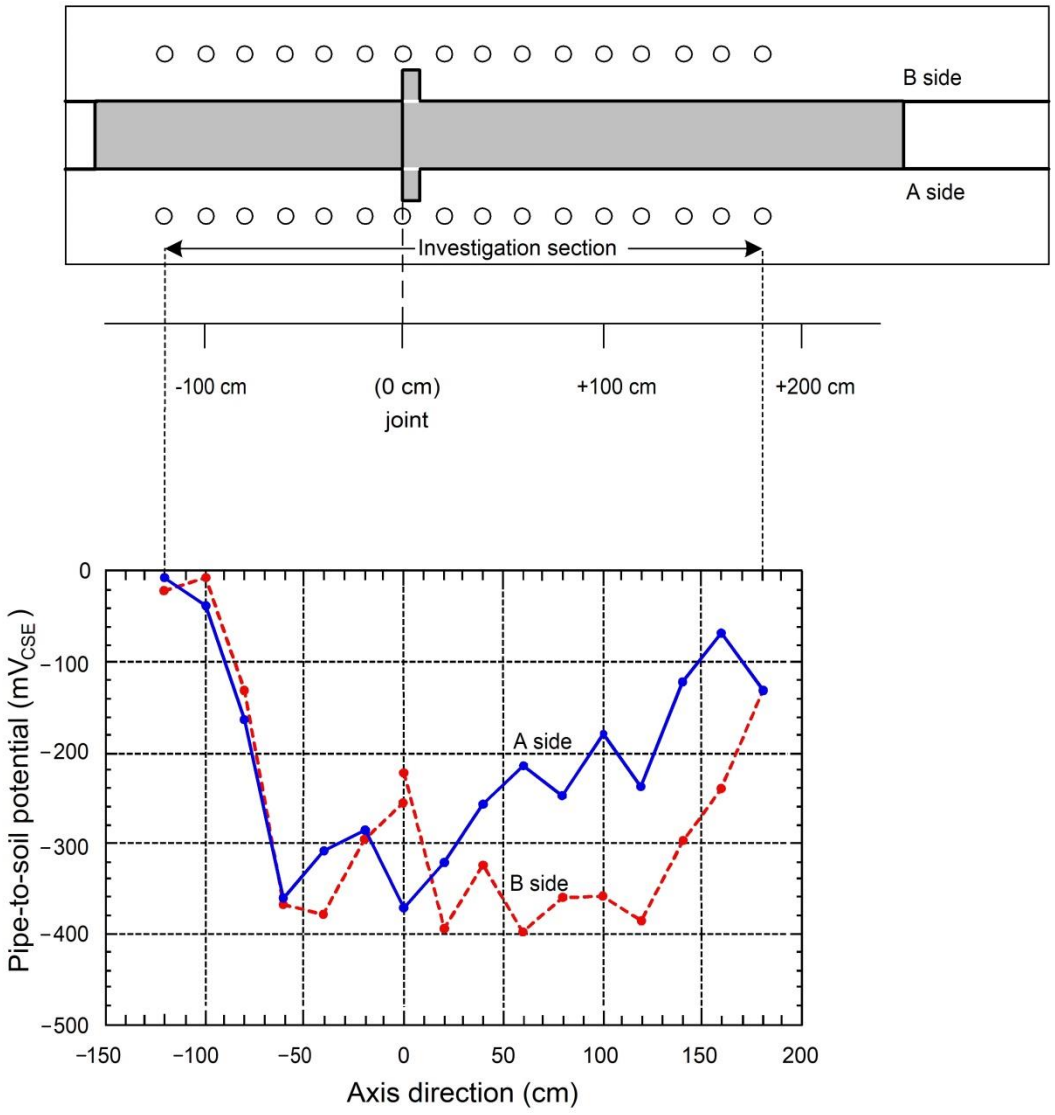

Figure 4 Close interval survey of pipe-to-soil potential on both sides of the pipeline.

Figure 5 shows the investigated ductile-iron pipeline. Figure 6 is a closeup of a corrosion pit.

Figure 5 Natural gas low pressure 100 mm diameter ductile-iron pipe in a d.c. stray current exposure area, before (above) and after removal of corrosion products and soil adhered to the pipe surface. This pipe had been in service for 14 years.

Figure 6 Close-up of a pit discovered at the point of 144,5 cm.
(Size: 6,5 mm×2,0 mm)

4.4.3 Microbiologically influenced corrosion

It has been recognized for a long time that sulfate-reducing bacteria are implicated in the soil corrosion process confined to anaerobic environments. However, from this investigation, it became clear in terms of microbially influenced corrosion that other microorganisms such as iron-oxidizing bacteria (acid-producing bacteria) and iron bacteria (tubercle-forming bacteria) were also implicated.

4.4.3.1 Iron-oxidizing bacteria-related corrosion (No. 40)

An investigation into a natural gas low pressure 200 mm diameter pipe (No. 40) was made. This pipe had been in service for 17 years buried in low resistivity (27,2 Ω m) acid sulfate soil containing aggressive sulfuric acid produced by high number of iron-oxidizing bacteria of 1×10^5 /g-soil, resulting in soil pH 3,82. Maximum corrosion rate of 0,405 mm/y was observed. In the case of ductile-iron pipelines buried in acid sulfate soil, they were subject to corrosivity of soil itself. Table 1 shows comparison of corrosion product and bulk soil of chemical and bacterial analysis results

Table 1 Comparison of corrosion product and bulk soil containing iron-oxidizing bacteria of chemical and bacterial analysis results.

		Corrosion product	Bulk soil
Corrosion potential of ductile-iron test specimen E_{corr} (V_{CSE})			−0,751
Resistivity (Ω m)			27,2
Water content W_c (%)			52,4
Eh (V_{SHE})		0,444	0,664
pH		5,70	3,82
Fe^{2+} (mass ppm)		2547	17
FeS (mass ppm)		766	90
SO_4^{2-} (mass ppm)			518
NO_3^- (mass ppm)			6
Cl^- (mass ppm)			74
Organic acid (mass ppm)	Formic acid	ND	ND
	Acetic acid	ND	ND
	Propionic acid	ND	ND
	Lactic acid	ND	2
	Pyruvic acid	ND	ND
	Butyric acid	ND	ND
Bacterial counts (/g)	SRB	1×10^4	1×10^2
	IOB	4×10^2	1×10^5
	SOB	4×10	0

ND = not detected

Less negative corrosion potential of ductile-iron test specimen of −0,751 V_{CSE} was observed, indicating aerobic environment.
It should be noted that the decrease in redox potential and increase in pH of corrosion product compared to bulk soil indicated the depletion of dissolved oxygen by aerobic iron-oxidizing bacteria and sulfuric acid at pipe/soil interface. This is the reason why SRB counts of corrosion product increased by two order magnitude than bulk soil.

Iron-oxidizing bacteria (IOB) (e.g., *Thiobacillus ferrooxidans*) grow in aerobic conditions with low pH and a large amount of SO_4^{2-} and produce aggressive H_2SO_4.
Silverman and Lundgren reported that the molecular ratio of ferrous ions oxidized to oxygen used is 4:1 in the presence of active iron-oxidizing bacteria as shown in equation (3)[3]:

$$4FeSO_4 + O_2 + 10H_2O \rightarrow 4Fe(OH)_3 + 4H_2SO_4 \quad (3)$$

Therefore, IOB are categorized as acid-producing bacteria (APB).
By taking the above-mentioned into account, possible corrosion processes influenced by IOB are as follows:

$Fe \rightarrow Fe^{2+} + 2e^-$	anodic reaction	(4)
$Fe^{2+} + SO_4^{2-} \rightarrow FeSO_4$	provision of the substrate for IOB	(5)
$FeSO_4 + 1/4O_2 + H_2O \xrightarrow{IOB} 1/2Fe(OH)_3 + 1/4Fe_2(SO_4)_3 + 1/4H_2SO_4$	oxidation of Fe^{2+} to Fe^{3+} by IOB	(6)
$1/4Fe_2(SO_4)_3 + 1/4Fe \rightarrow 3/4FeSO_4$	chemical attack on Fe	(7)
$2H^+ + 1/2O_2 + 2e^- \rightarrow H_2O$	cathodic reaction	(8)

Concentration of dissolved oxygen and sulfuric acid decreased with time by the action of iron-oxidizing bacteria and cathodic reaction, resulting in decrease in redox potential and increase in pH at pipe/soil interface as shown in Table 1..

4.4.3.2 Sulfate-reducing bacteria-related corrosion

Figure 7 shows natural gas low pressure 150 mm diameter ductile-iron pipe buried in low resistivity (17,7 Ω m) anaerobic soil containing sulfate-reducing bacteria (SRB), before (above) and after (below) removal of corrosion products and soil adhered to the pipe surface. This pipe had been in service for 16 years. The ductile-iron pipeline that was exposed under fully anaerobic conditions (bulk soil Eh = −0,001 V_{SHE})

experienced relatively low corrosion rate of 0,20 mm/y despite the presence of high concentration of SRB, 1×10^4 /g-soil. Corrosion product was soft and black.

Sulfate-reducing bacteria (SRB, e.g., *Desulfovibrio desulfuricans*) reduce inorganic sulfate to sulfide at pH 5,5 to 8,5 under anaerobic conditions. In 1931, Stephenson and Stickland reported that the molecular ratio of sulfate ions reduced to hydrogen used is 1:4 in the presence of active SRB at pH 7,4 according to the following equation[4]:

$$SO_4^{2-} + 4H_2 \rightarrow S^{2-} + 4H_2O \quad (9)$$

Figure 7 Natural gas low pressure 150 mm diameter ductile-iron pipe in anaerobic soil containing sulfate-reducing bacteria, before (above) and after (below) removal of corrosion products and soil adhered to the pipe surface. This pipe had been in service for 16 years.

Table 2 shows comparison of corrosion product and bulk soil of chemical and bacterial analysis results. The values of pH and ferrous ion concentration of corrosion product have increased compared to those of bulk soil, with a consequent decrease in redox potential as shown in equation (2). The properties of the corrosion product varied with time because of bacterial action. Iron sulfide concentration of corrosion product was higher than that of bulk soil by about twentyfold. This indicates that SRB were implicated in the corrosion process under fully anaerobic and neutral pH conditions. Soils contained large amounts of lactic acid, 62 mass ppm, as nutrients of SRB necessary for high numbers of these bacteria.

Table 2 Comparison of corrosion product and bulk soil containing sulfate-reducing bacteria of chemical and bacterial analysis results.

Factor		Corrosion product	Bulk soil
Resistivity (Ω m)			17,7
Water content W_c (%)			61.0
Eh (V_{SHE})		−0,161	−0,001
pH		7,20	6,00
Fe^{2+} (mass ppm)		2610	1350
FeS (mass ppm)		13385	645
SO_4^{2-} (mass ppm)			147
NO_3^- (mass ppm)			ND
Cl^- (mass ppm)			12
Organic acid (mass ppm)	Formic acid	7	ND
	Acetic acid	4	ND
	Propionic acid	ND	ND
	Lactic acid	9	62
	Pyruvic acid	ND	ND
	Butyric acid	ND	ND
Bacterial counts (MPN/g)	SRB	1×10^4	1×10^4
	IOB	0	0
	SOB	7×10^3	4×10

ND = not detected

Figure 8 shows the transvers section of 10,9 mm wall thickness ductile-iron pipe and microstructure at the most severe corrosion site. As shown in Figure 8, graphitic corrosion was observed for a ductile-iron pipe. No corrosion was observed on the inner surface of the pipeline, because of no corrosive natural gas flowing.

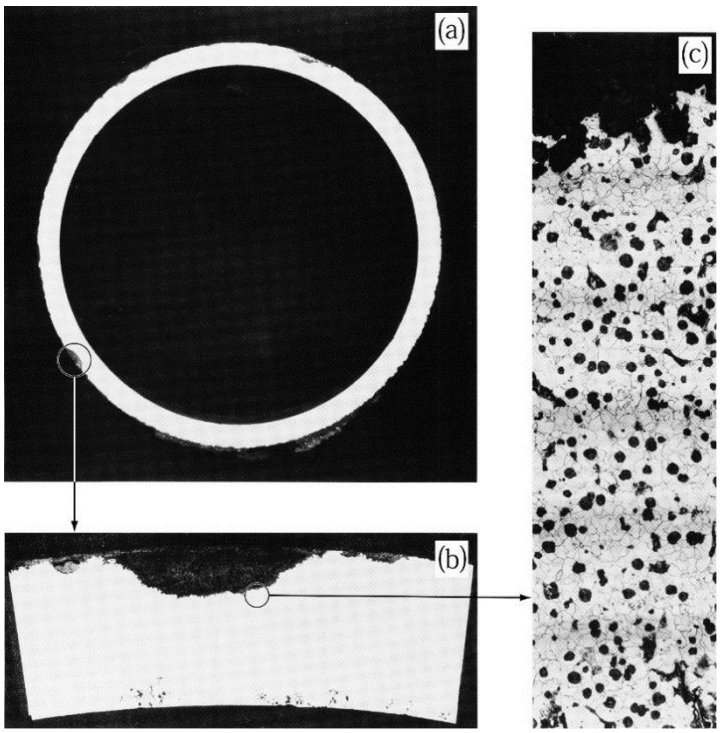

Figure 8 Graphitic corrosion of 10,9 mm depth ductile-iron and metallic structure.
(a) transverse section of 10,9 mm wall thickness of ductile-iron pipe
(b) close-up of graphitic corrosion
(c) microstructure of ductile-iron

Figure 9 shows X-ray diffraction pattern of the analyzed corrosion product. Unoxidized siderite and iron sulfides such as greigite and marcasite were present on the outer surface of the pipe. Quartz was a soil component.

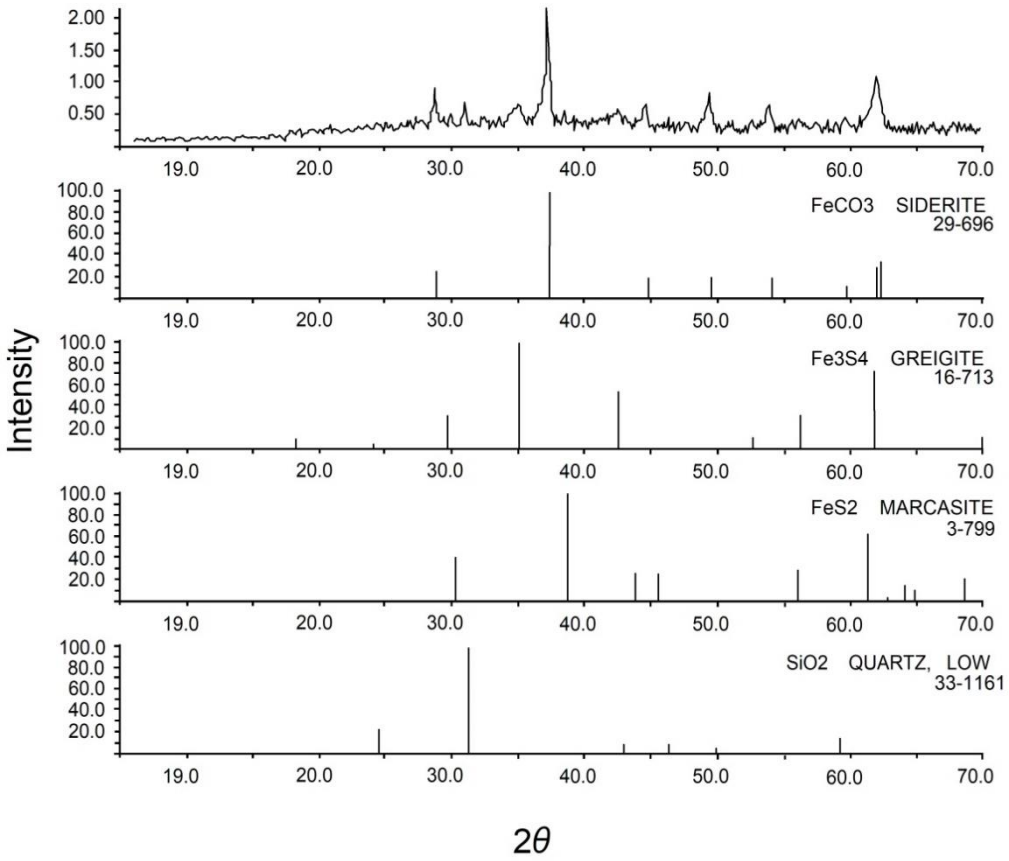

Figure 9 X-ray diffraction pattern of the sampled corrosion products.

In the anaerobic corrosion process of iron, black iron sulfides and white siderite are the major corrosion products.

By taking the action of sulfate-reducing bacteria shown by equation (9) and the properties of corrosion product, corrosion was thought to proceed according to the following stages:

<In the early stages>

$Fe \rightarrow Fe^{2+} + 2e^-$	anodic reaction	(10)
$1/2O_2 + H_2O + 2e^- \rightarrow 2OH^-$	cathodic reaction	(11)
$Fe^{2+} + 2OH^- \rightarrow Fe(OH)_2$	corrosion product	(12)

<In the later stages>

$4Fe \rightarrow 4Fe^{2+} + 8e^-$	anodic reaction	(13)
$8H_2O + 8e^- \rightarrow 4H_2 + 8OH^-$	cathodic reaction	(14)
SRB	reduction of SO_4^{2-} to S^{2-}	
$SO_4^{2-} + 4H_2 \rightarrow S^{2-} + 4H_2O$	by SRB	(15)
$Fe^{2+} + S^{2-} \rightarrow FeS$	corrosion product	(16)
$(3 - x)\ Fe^{2+} + (6 - 2X)\ OH^- \rightarrow (3 - x)\ Fe(OH)_2$	corrosion product	(17)

$X\ CO_2 + x\ H_2O \rightarrow x\ H_2CO_3$	Dissolution in water of CO_2	(18)
$X\ H_2CO_3 \rightarrow x\ H^+ + x\ HCO_3^-$	dissociation of H_2CO_3	(19)
$X\ HCO_3^- \rightarrow x\ H^+ + x\ CO_3^{2-}$	dissociation of HCO_3^-	(20)
$4Fe + (4 - x)\ H_2O + SO_4^{2-} + x\ CO_2$ $\rightarrow FeS + (3 - x)\ Fe(OH)_2 + x\ FeCO_3 + 2OH^-$	Overall reaction	(21)

4.4.3.3 Iron bacteria-related corrosion

Figure10 shows natural gas low pressure 150 mm diameter ductile-iron pipe in sandy marine sediments containing a large amount of HCO_3^- ions, 456 mass ppm. This pipe had been in service for 17 years. Maximum corrosion rate was 0,384 mm/y. Tubercle was formed on the pipe surface, presumably due to the action of iron bacteria.

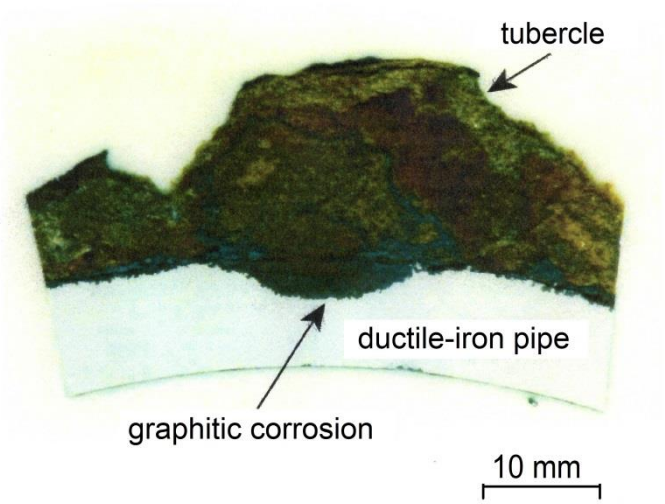

Figure 10 Natural gas low pressure 150 mm diameter ductile-iron pipe in sandy marine sediments containing a large amount of HCO_3^- ions, 456 mass ppm. This pipe had been in service for 17 years.

Iron bacteria oxidize (IB, e.g., *Gallionella*, *Leptothrix* etc.) soluble ferrous ions to ferric ions under neutral pH conditions with the consequent precipitation and accumulation of ferric hydroxide on the external surfaces of the gas pipes. The area beneath the tubercle becomes the anaerobic site which sustains severe graphitic corrosion. Corrosion sites develop under the growing tubercle.

Table 3 shows chemical and bacterial analysis results of bulk soil.

Table 3 Chemical and bacterial analysis results of bulk soil.

Factor		Bulk soil
Corrosion potential of ductile-iron test specimen E_{corr} (V_{CSE})		−0,684
Resistivity (Ωm)		56,6
Water content W_c (%)		22,2
Eh (V_{SHE})		399
pH		8,88
Fe^{2+} (mass ppm)		19
FeS (mass ppm)		111
SO_4^{2-} (mass ppm)		82
NO_3^- (mass ppm)		1
Cl^- (mass ppm)		8
HCO_3^- (mass ppm)		456
Organic acid (mass ppm)	Formic acid	ND
	Acetic acid	ND
	Propionic acid	ND
	Lactic acid	ND
	Pyruvic acid	ND
	Butyric acid	ND
Bacterial counts (/g)	SRB	2×10^3
	IOB	0
	SOB	0

ND = not detected

Baylis reported that ferrous carbonate and calcium carbonate are insoluble compounds but that their solubility increases in the presence of bicarbonate ions, HCO_3^-[5]. Possible iron bacteria-related corrosion processes are as follows:

$Fe \rightarrow Fe^{2+} + 2e^-$ anodic reaction (22)

$1/2O_2 + H_2O + 2e^- \rightarrow 2OH^-$ cathodic reaction (23)

$Fe^{2+} + 2OH^- \rightarrow Fe(OH)_2$ production of $Fe(OH)_2$ (24)

$Fe(OH)_2 + 2HCO_3^- \rightarrow Fe(CO_3)_2^{2-} + 2H_2O$ dissolution of $Fe(OH)_2$ (25)

IB

$Fe(CO_3)_2^{2-} + 1/4O_2 + 3/2H_2O \rightarrow FeOOH + 2HCO_3^-$ production of tubercle FeOOH and HCO_3^- (26)

The process of anaerobic digestion of organic matters produces a large amount of

carbon dioxide. The carbon dioxide in the soil from decaying organic matter readily dissolves in the high pH electrolyte such as groundwater, producing a concentrated mixture of bicarbonate and carbonate in the pH range of 8 to 12.
Bicarbonate ions produced by equation (19) will contribute to dissolve insoluble ferrous carbonate (equation (25)), with the consequent formation and accumulation of tubercle (equation (26)).

5 Conclusions

1) Graphitic corrosion of ductile-iron pipelines can occur at any pH, although different rates of that corrosion were observed.
2) Corrosion fell into three divisions roughly according to pH range of soil, that is, 1) acid corrosion caused by iron-oxidizing bacteria at pH below 5, 2) sulfate-reducing bacteria corrosion at pH 5 to 9,5, and 3) HCO_3^-−CO_3^{2-}corrosion at pH 8 to 12. It was considered that insoluble iron hydroxide formed on a surface dissolved by a significant amount of HCO_3^-, resulting in corrosion at pH above 8 in aerobic soils.
3) Stray-current corrosion was observed in a d.c. stray current exposure area.

References

[1] F. Kajiyama, “A doctoral thesis,” Tokyo Institute of Technology (1989)
[2] F. Kajiyama, “Soil redox potential in consideration of thermodynamics and properties,” Bõsei Kanri, 62, 12, p.450−453 (2018) in Japanese
[3] M. P. Silverman, D. G. Lundgren, “Studies on the chemoautotrophic iron bacterium *Thiobacillus Ferrooxidans*,”Journal of Bacteriology, 78, p.326−331 (1959)
[4] M. Stephenson, L. H. Stickland,“ XXⅧ. Hydrogenase. Ⅱ. The reduction of sulphate to sulphide by molecular hydrogen,” Biochemical journal, 25, p.215−220 (1931)
[5] J. R. Baylis, “Factors other than dissolved oxygen influencing the corrosion of iron pipes, “ Ind. Eng. Chem. 18, 370 (1926).